

Effective Fine-Tuning of Vision-Language Models for Accurate Galaxy Morphology Analysis

Ruoqi Wang
HKUST(GZ)

rwang280@connect.hkust-gz.edu.cn

Haitao Wang
SYSU

wanght39@mail2.sysu.edu.cn

Qiong Luo
HKUST(GZ) & HKUST

luo@cse.ust.hk

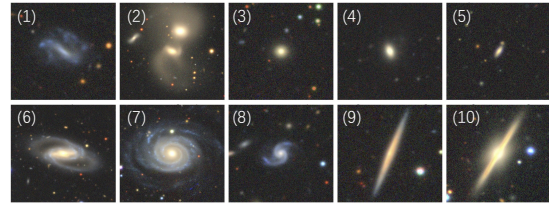
Abstract

Galaxy morphology analysis involves classifying galaxies by their shapes and structures. For this task, directly training domain-specific models on large, annotated astronomical datasets is effective but costly. In contrast, fine-tuning vision foundation models on a smaller set of astronomical images is more resource-efficient but generally results in lower accuracy. To harness the benefits of both approaches and address their shortcomings, we propose GalaxAlign, a novel method that fine-tunes pre-trained foundation models to achieve high accuracy on astronomical tasks. Specifically, our method extends a contrastive learning architecture to align three types of data in fine-tuning: (1) a set of schematic symbols representing galaxy shapes and structures, (2) textual labels of these symbols, and (3) galaxy images. This way, GalaxAlign not only eliminates the need for expensive pretraining but also enhances the effectiveness of fine-tuning. Extensive experiments on galaxy classification and similarity search demonstrate that our method effectively fine-tunes general pre-trained models for astronomical tasks by incorporating domain-specific multi-modal knowledge.

1. Introduction

Galaxy morphology analysis involves studying galaxies based on their shapes and structures. This information is crucial for understanding galaxy formation and evolution, and it can be conveyed through natural language and schematic diagrams of galaxy images [16, 29]. As shown in Figure 1, schematic symbols paired with textual labels effectively capture the distinct characteristics of individual galaxies [3, 4]. These textual descriptions and schematic diagrams have proven useful in guiding amateur volunteers in galaxy image annotation [29]. In this paper, we explore how this multi-modal information can enhance foundation models for galaxy morphology analysis.

Foundation models pre-trained on large-scale natural im-



(a) Examples of galaxy images.



(b) Examples of galaxy morphology description and schematic symbols corresponding to the images in subfigure (a).

Figure 1. Examples of galaxy images, corresponding schematic symbols and their textual labels. Images and textual labels are from the Galaxy10 DECaLS dataset [11], whereas schematic symbols are from the Galaxy Zoo 2 decision tree [7, 34].

age datasets, such as ImageNet [21], perform well in various multimedia applications. However, researchers commonly believe that these pre-trained models are insufficient for astronomical images [24, 27, 31]. This concern arises because the domain-specific scientific data differ significantly from the general natural image datasets used for foundation models, leading to distribution shifts that reduce the effectiveness of these models when applied directly to galaxy analysis [27].

As a result, astronomical foundation models have typically relied on pretraining with large-scale astronomical datasets [7, 15, 16, 34]. These models are trained from scratch using extensive domain-specific datasets and subsequently fine-tuned for downstream tasks, overlooking the potential benefits of adapting publicly available vision foundation models that are pre-trained on natural datasets.

Moreover, annotating galaxy images heavily depends on the efforts of experts and volunteers, requiring significant human resources and time [14, 15, 29]. Therefore, there is a pressing need for a method that reduces reliance on large domain-specific datasets and directly utilizes readily available pre-trained models trained on natural image data.

Based on the above observations, this work aims to investigate whether a galaxy model extended from pre-trained foundation models on natural image data can reduce the reliance on large astronomical datasets. To address this need, we introduce **GalaxAlign**, a tri-modal fine-tuning framework that adapts pre-trained CLIP models [20] for galaxy morphology analysis by integrating schematic symbols, textual descriptions, and galaxy images. Since human amateur volunteers can label astronomical images based on their knowledge learned from textual descriptions and schematic diagrams, we believe that these modalities can also assist models pre-trained on general datasets in performing classification tasks on astronomical images.

Specifically, GalaxAlign employs a two-stage fine-tuning approach: In the first stage, galaxy images and schematic symbols are input into a shared image encoder, while textual descriptions are processed by a separate text encoder. This stage enables the image encoder to learn a shared representation of galaxy features from both symbolic and photographic images. In the second stage, GalaxAlign transfers the parameters from the shared encoder in Stage 1 to initialize a separate symbol encoder, enabling each encoder to specialize in a single modality—images, symbols, or text. This parameter transfer leverages the shared encoder’s foundational understanding of galaxy morphology, learned from both images and schematic symbols in Stage 1, as a strong starting point for Stage 2. The second stage fine-tuning aligns each modality for more precise feature embedding by focusing each encoder on its unique input.

This tri-modal alignment enhances the model’s ability to distinguish detailed structural features, improving classification and similarity search accuracy without costly large-scale pretraining. Extensive experiments show that GalaxAlign effectively fine-tunes pre-trained models, achieving high accuracy in astronomical tasks by incorporating domain-specific multi-modal knowledge.

Our contributions are as follows:

- Our method effectively extends models pre-trained on natural images for astronomical tasks, eliminating the need for large-scale astronomical datasets.
- We reduce reliance on manually labeled data, providing a novel solution for galaxy morphology tasks.
- We present a multi-modal learning architecture that incorporates text and symbols to adapt models pre-trained on general image datasets for use with galaxy images.

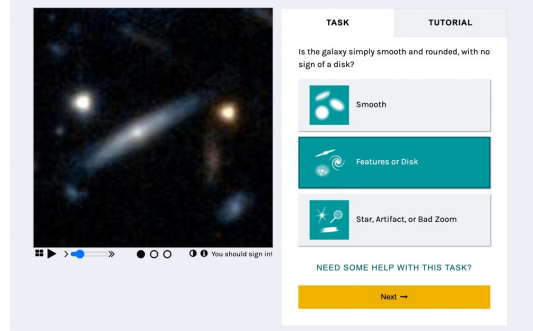


Figure 2. Multi-modal annotation instructions for volunteers [35].

2. Background and Related Work

2.1. Foundation Models in Astrophysics

Unlike natural images, astrophysics images tend to have the following properties [27]:

- **Sparseness:** Objects occupy only a small fraction of each image.
- **Noise:** Systematic noise is present in the images.
- **High Dynamic Range:** Object brightness spans several orders of magnitude.
- **Artifacts:** Instrumental effects or reconstruction residuals introduce unintended structures of various scales.

Due to these differences, astronomers regard general vision models trained on natural images as inadequate for astronomical tasks. As such, instead of fine-tuning existing vision foundation models to fit astronomical data, Walmsley et al. proposed a galaxy morphology foundation model pre-trained on large-scale galaxy morphology datasets [31]. However, constructing such datasets is time-consuming and labor-intensive. For instance, the GZD-5 project, which classified 262,000 galaxies, spanned over three years from March 2017 to October 2020 [30]. Similarly, in the recent Galaxy Zoo campaign, 38,949 volunteers annotated a total of 105,000 galaxies over nearly two years (November 2020 to October 2022) [33].

To reduce the amount of time and labor required for creating large, labeled astronomical datasets, an alternative approach is to adapt existing foundation models pre-trained on natural images to astronomical tasks. Some representative pre-trained general vision foundation models including DINOv2 [19], MAE [10], MSN [1], supervised ResNet [9], and supervised ViT [8], have been fine-tuned to adapt to galaxy morphology tasks. However, their performance is generally poor [27]. These results suggest that adapting vision foundation models for astrophysics applications requires further considerations of data characteristics and alignment with domain-specific knowledge. Our work contributes to this effort.

2.2. Citizen Science and Multi-Modal Data

Citizen science projects are the primary method for large-scale galaxy morphology annotation. In the Galaxy Zoo projects [16, 30, 34], volunteers annotate astronomical images based on specific instructions. This process heavily relies on providing amateur volunteers with simplified schematic symbols and natural language descriptions to guide them through the classification process.

Figure 2 illustrates an example of the annotation guidance available to volunteers on the Galaxy Zoo online platform [35]. Volunteers are presented with symbols that depict different morphological features, such as spiral arms, bars, or mergers, accompanied by concise textual descriptions of these features. In this annotation process, the combination of visual symbols and natural language descriptions helps non-experts connect their common sense with astronomical knowledge, enabling them to effectively complete labeling tasks.

Inspired by this approach, our method integrates schematic symbols and natural language descriptions as key components in galaxy morphology tasks, aiming to bridge the gap between pre-trained general models and astronomical data.

2.3. Multi-Modal Contrastive Learning Models

Vision-language models, such as CLIP [20], utilize contrastive learning to align visual and textual embeddings. These models obtain strong generalization capabilities by training on large-scale datasets that pair images with corresponding textual descriptions. Bowles et al. [3, 4] proposed a method to connect radio galaxy images with human-generated natural language descriptions to derive semantic morphology classes for classification, demonstrating that textual descriptions can align with distinct identifying features in the images [18].

Moreover, multi-modal contrastive learning has been widely applied in various scientific domains [13, 15, 17, 18, 22, 26], learning semantic representations effectively across diverse modalities. In this paper, we present the first application of associating astronomical data with three modalities—images, text, and schematic symbols—demonstrating that contrastive learning can effectively align these modalities.

3. Method

We introduce GalaxAlign, a tri-modal learning framework based on the CLIP architecture, for galaxy morphology tasks by incorporating and aligning three modalities: textual descriptions, astronomical images, and schematic symbols. Our approach contains three encoders: a text encoder for textual labels, an image encoder for galaxy images, and a symbol encoder for schematic symbols. Our finetuning

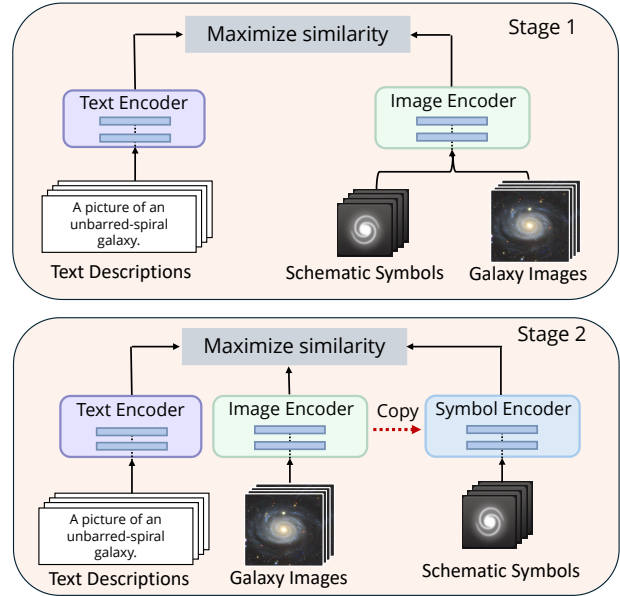


Figure 3. Overview of our GalaxAlign. Stage 1 is the initial finetuning with schematic symbols and images sharing a single encoder. Stage 2 is the finetuning with three separate encoders.

is conducted in two stages: (1) Symbol-Image with Text Training and (2) Tri-modal Joint Training.

Our framework contains three encoders:

- **Text Encoder:** It processes textual descriptions related to galaxy morphology.
- **Image Encoder:** Initially it encodes both galaxy images and schematic symbols. In the second stage, the image encoder encodes galaxy images only.
- **Symbol Encoder:** It is derived from the Image Encoder after the first stage to encode schematic symbols in the second stage.

3.1. Textual Description

Our input text follows the common format *A picture of a/an {class name}*. Since the *class name* clearly and concisely describes the structure of the galaxies, it provides an efficient and identifying textual label. For example, sentences such as “A picture of an unbarred-spiral galaxy” or “A picture of a cigar round smooth galaxy” effectively capture the structural information of the galaxies.

3.2. Stage 1: Symbol-Image with Text Training

In the first stage, the Image Encoder takes both galaxy images and symbols as its input, whereas the Text Encoder processes corresponding text descriptions. This stage aligns the representations of images and symbols with text descriptions, setting up a shared multi-modal embedding space. The shared Image Encoder extracts patterns in galaxy shapes and structures that are consistent across sym-

bols and images. Both encoders are initialized with pre-trained weights of the CLIP model [12] on natural images.

For each input galaxy image x_{img} , schematic symbol x_{sym} , and text description x_{txt} , we obtain embeddings:

$$z_{\text{img}} = E_{\text{img}}(x_{\text{img}}), \quad z_{\text{sym}} = E_{\text{img}}(x_{\text{sym}}), \quad z_{\text{txt}} = E_{\text{txt}}(x_{\text{txt}})$$

To align image/symbol and text embeddings, we use a contrastive loss function that maximizes the cosine similarity between positive (matching) pairs and minimizes it for non-matching pairs. For batch size N , the loss function for image-text and symbol-text pairs is:

$$\mathcal{L}_{\text{con}} = -\frac{1}{2N} \sum_{i=1}^N \left(\log \frac{\exp(\text{sim}(z_{\text{img/sym}}^i, z_{\text{txt}}^i)/\tau)}{\sum_{j=1}^N \exp(\text{sim}(z_{\text{img/sym}}^i, z_{\text{txt}}^j)/\tau)} \right)$$

where $\text{sim}(z_a, z_b)$ denotes the cosine similarity and τ is a learnable temperature parameter.

In our method, **Stage 1 serves as a warm-up phase** rather than full-convergence training. Empirically, we found that training for just over 10 epochs in our experiments was sufficient to achieve optimal results, eliminating the need for full convergence at this stage. This approach allows the model to establish a solid foundation for galaxy morphology analysis without excessive computation in the initial stage.

3.3. Stage 2: Tri-Modal Joint Training

In Stage 2, we transition from a shared encoder to separate, modality-specific encoders, allowing the encoders to refine and specialize in the unique features of images, symbols, and text individually. To facilitate this specialization, we copy the parameters from the shared image encoder E_{img} from Stage 1 to initialize the symbol encoder E_{sym} :

$$E_{\text{sym}} \leftarrow E_{\text{img}}$$

With the symbol encoder starting from the same representation as the image encoder, both encoders are more likely to produce embeddings that are well-aligned in the feature space. Moreover, rather than learning from scratch, the symbol encoder refines and specializes existing representations from Stage 1, allowing itself to capture modality-specific details more quickly.

All three encoders are then fine-tuned together, optimizing the alignment across text, image, and symbol representations. The resulting embeddings are:

$$z_{\text{img}} = E_{\text{img}}(x_{\text{img}}), \quad z_{\text{sym}} = E_{\text{sym}}(x_{\text{sym}}), \quad z_{\text{txt}} = E_{\text{txt}}(x_{\text{txt}})$$

The Stage 2 loss function includes three contrastive components to ensure effective alignment across all three modalities. We define the modality pairs as:

$$(a, b) \in \{(\text{img}, \text{txt}), (\text{img}, \text{sym}), (\text{sym}, \text{txt})\}$$

For each pair, the contrastive loss is computed as:

$$\mathcal{L}_{\text{total}} = -\frac{1}{N} \sum_{i=1}^N \sum_{(a,b)} \log \frac{\exp(\text{sim}(z_a^i, z_b^i)/\tau)}{\sum_{j=1}^N \exp(\text{sim}(z_a^i, z_b^j)/\tau)}$$

This loss function facilitates a balanced alignment across the three modalities, enabling the model to jointly learn textual descriptions, visual images, and schematic symbols for galaxy morphology tasks.

4. Experiments

4.1. Experimental Setup

4.1.1 Platform

We conduct all experiments on a server with two AMD EPYC 7543 CPUs, 512GB main memory, and four NVIDIA RTX A6000 GPUs each with 48GB device memory. The operating system is Ubuntu 22.04. Our model is implemented in PyTorch 2.1.0.

4.1.2 Datasets

In our experiments, we evaluate our method on two representative public galaxy datasets: (1) Galaxy10 DECaLS [11] and (2) GalaxyMNIST [28]. Galaxy10 contains 17,736 colored galaxy images divided in 10 classes, with each image of a size 256×256 pixels. This dataset is from the DESI Legacy Imaging Surveys [6], which merges data from the Beijing-Arizona Sky Survey (BASS) [36], the DECam Legacy Survey (DECaLS) [2], and the Mayall z-band Legacy Survey [23]. In comparison, GalaxyMNIST [28], derived from Galaxy Zoo DECaLS [30], contains 10,000 galaxy images (64×64) of four morphological classes.

4.1.3 Evaluation Metrics

In this study, we evaluate the performance of GalaxAlign on classification tasks using Accuracy and F1 Score (macro). For the similarity search task, we use mean Average Precision (mAP), which reflects the ranking quality by calculating the average precision at various recall levels for each query and then averaging across all queries.

4.1.4 Methods under Comparison

We evaluate GalaxAlign with the state-of-the-art foundation models, including mainstream general vision models and specialized astronomical foundation models trained on large-scale domain-specific datasets. The baseline models include:

- **MAE** [10], **DINOv2** [19], **MSN** [1]: Vision foundation models using self-supervised pretraining techniques. Following Lastufka et al. [27], we fine-tune the models using galaxy datasets of variant sizes in downstream tasks.

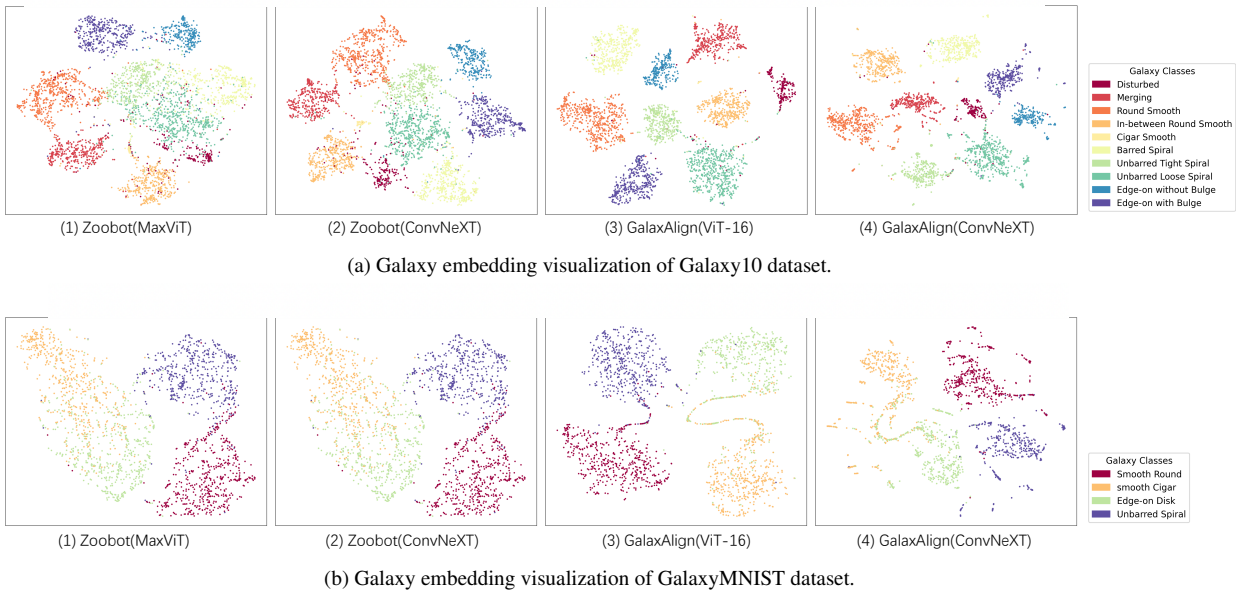


Figure 4. The t-SNE visualization for features extracted using Zoobot (MaxViT and ConvNeXT) and GalaxAlign (ViT-16 and ConvNeXT) on Galaxy10 and GalaxyMNIST datasets.

- **ViT-16** [8], **ResNet-50** and **ResNet-18** [9]: Standard vision models pretrained on ImageNet-1k [9] with a supervised method for classification.
- **Zoobot** [32]: State-of-the-art astronomical models, pretrained specifically on large scale galaxy data from scratch. We selected MaxViT and ConvNeXT as the backbone networks for Zoobot because they performed the best among all backbones [32].

Table 1. Models used in our comparison study.

Model Name	Backbone	Pre-training Dataset
MAE [10]	ViT-Base/16	ImageNet-1k [5]
DINOv2 [19]	ViT-Base/14	LVD-142M [19]
MSN [1]	ViT-Base/16	ImageNet-1k [5]
ViT-16 [8]	ViT-Base/16	ImageNet-1k [5]
ResNet 50 [9]	ResNet 50	ImageNet-1k [5]
ResNet 18 [9]	ResNet 18	ImageNet-1k [5]
Zoobot [32]	MaxViT-Base	GZ DECaLS GZD-5 [30]
	ConvNeXT-Base	GZ DECaLS GZD-5 [30]

4.2. Feature Projections

To demonstrate GalaxAlign’s strong performance without relying on extensive domain-specific datasets, We present the embedding visualization comparing our method with Zoobot, which has been pretrained on large astronomical datasets and then fine-tuned on smaller datasets. Figure 4 provides a t-SNE visualization [25] of galaxy data embeddings learned by different models. Feature embeddings of other baseline methods are presented in the appendix.

In Figure 4 (a), both Zoobot models (MaxViT and ConvNeXT) display notable overlaps between complex classes including Barred Spiral Galaxy, Unbarred Tight Spiral and Unbarred Loose Spiral, indicating limited effectiveness in distinguishing fine morphological details. In contrast, our GalaxAlign models (ViT-16 and ConvNeXT) exhibit well-separated, clearly defined clusters with minimal overlap, demonstrating effectiveness in category distinction and feature representation. Meanwhile, GalaxAlign consistently maintains distinct clusters across all categories, reflecting its ability to capture essential morphological features accurately. In Figure 4 (b), Zoobot models exhibit some clustering but display considerable overlap in the Smooth Cigar and Edge-on Disk categories. In contrast, GalaxAlign models achieve more distinct, well-separated clusters across all categories. Overall, these results highlight GalaxAlign’s advantage over Zoobot in achieving compact intra-class clustering and distinct inter-class separability, underscoring its effectiveness in representing galaxy morphology.

Figure 5 shows a 2D grid visualization of galaxy images sampled from the GalaxyMNIST dataset, where high-dimensional features are reduced using PCA and aligned to a grid. The clusters and smooth transitions between similar galaxy types in the grid suggest that our model effectively encodes structural information in the feature space, allowing visually similar galaxies to occupy nearby regions. The visualization of images in the Galaxy10 dataset is presented in the appendix.

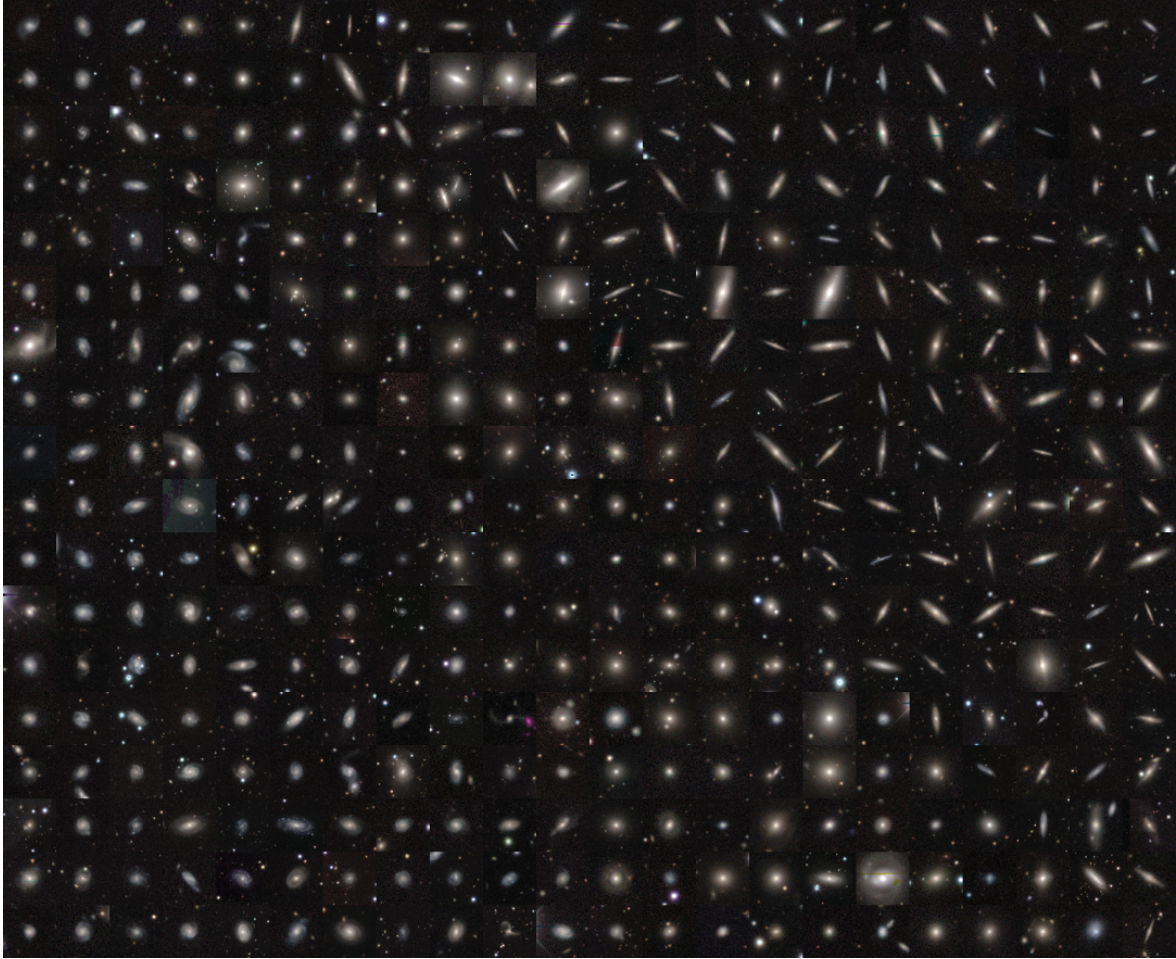


Figure 5. Visualisation of the representations learned by our method, illustrating similar galaxies occupying nearby regions in the feature space. This visualization is created using PCA to compress the representation to 2D and placing galaxy thumbnails at the locations of their corresponding galaxies in the grid.

Table 2. Comparison of Classification Performance (mean and standard deviation) on GalaxyMNIST and Galaxy10

Method	Pretraining Dataset		GalaxyMNIST		Galaxy10	
	General	Domain	Accuracy	F1 Score	Accuracy	F1 Score
MAE	✓		0.7312 (0.0070)	0.7314 (0.0069)	0.6242 (0.0041)	0.5990 (0.0098)
DINOv2	✓		0.8786 (0.0013)	0.8789 (0.0014)	0.8465 (0.0008)	0.8337 (0.0010)
MSN	✓		0.8275 (0.0016)	0.8279 (0.0017)	0.6113 (0.0030)	0.5616 (0.0032)
ViT-16	✓		0.8519 (0.0021)	0.8521 (0.0021)	0.7304 (0.0007)	0.7054 (0.0015)
ResNet-18	✓		0.8720 (0.0150)	0.8722 (0.0151)	0.9501 (0.0123)	0.9446 (0.0117)
ResNet-50	✓		0.8877 (0.0059)	0.8884 (0.0059)	0.9466 (0.0023)	0.9399 (0.0040)
Zoobot (MaxViT)		✓	0.8790 (0.0022)	0.8796 (0.0023)	0.8922 (0.0065)	0.8847 (0.0066)
Zoobot (ConvNeXT)		✓	0.9360 (0.0009)	0.9365 (0.0009)	0.9600 (0.0061)	0.9550 (0.0062)
Ours (ViT-16)	✓		0.9272 (0.0005)	0.9276 (0.0004)	0.9732 (0.0004)	0.9702 (0.0005)
Ours (ConvNext)	✓		0.9372 (0.0015)	0.9377 (0.0015)	0.9710 (0.0014)	0.9664 (0.0008)

4.3. Galaxy Morphology Classification

Table 2 provides a comparative analysis of classification performance across different methods on the GalaxyMNIST and Galaxy10 datasets.

The self-supervised models (MAE [10], DINOv2 [19], and MSN [1]), when fine-tuned following Lastufka et al. [27], show promising performance on GalaxyMNIST but are generally outperformed by models pretrained with supervised learning [8, 9], particularly on Galaxy10. This re-

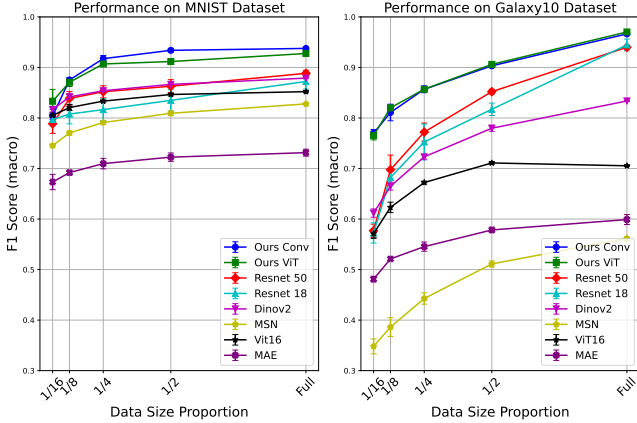


Figure 6. Performance Comparison of Different Methods on MNIST and Galaxy10 Datasets (F1 Score)

sult suggests that while self-supervised pretraining captures general features, supervised models pretrained on natural images, tend to transfer more effectively to the morphological distinctions in astronomical images.

The Zoobot models [32] (using MaxViT and ConvNeXT as the backbone network, respectively), specifically pretrained on large-scale galaxy data, demonstrate strong performance on both datasets. This result underscores the value of domain-specific pretraining for high-performance astronomical classification.

In contrast, our proposed models—Ours (ViT-16) and Ours (ConvNext)—pretrained on natural image datasets and fine-tuned using a multi-modal architecture that aligns textual descriptions, schematic symbols, and astronomical images, achieve comparable performance to Zoobot and outperform all other methods. These results highlight the effectiveness of adapting general pretrained models through multi-modal fine-tuning, providing an alternative to large-scale astronomical pretraining for galaxy morphology tasks.

Figure 6 compares the F1 scores of various models pretrained on natural data across different data sizes for the fine-tuning datasets, GalaxyMNIST and Galaxy10. Our models achieve the highest performance on both datasets, with all data sizes, showing efficient generalization and effective adaptation to astronomical tasks. Self-supervised models (e.g., DINOv2 [19], MAE [10], MSN [1]) and standard supervised models (e.g., ResNet-18, ResNet-50 [9] and ViT [8]) achieve moderate results, indicating that pretraining with natural image alone may not fully capture the domain-specific details required for astronomical tasks. These results illustrate the effectiveness of our multi-modal adaptation strategy in bridging general pretrained models and domain-specific applications in astronomy.

Table 3. Comparison of Mean Average Precision (mAP) on GalaxyMNIST and Galaxy10.

Method	GalaxyMNIST		Galaxy10	
	mAP@5	mAP	mAP@5	mAP
MAE	0.5867	0.2571	0.5592	0.1302
DINOv2	0.6472	0.2566	0.6193	0.1261
MSN	0.6372	0.3005	0.5569	0.1508
ViT-16	0.7929	0.4208	0.6800	0.2229
ResNet-18	0.9160	0.6865	0.9398	0.5827
ResNet-50	0.9184	0.6657	0.8732	0.5431
Zoobot (MaxViT)	0.9011	0.8408	0.9370	0.7842
Zoobot (ConvNeXT)	0.9406	0.9123	0.9491	0.8492
Ours (ViT-16)	0.9524	0.8865	0.9919	0.9645
Ours (ConvNeXT)	0.9569	0.9123	0.9868	0.9640

4.4. Similarity Search

In astronomy, automatically identifying the similarity between two galaxies is a challenging but essential task [31]. Effective searches for similar galaxies can help us find counterparts of rare galaxies, making the leap from a one-off discovery to a new class of phenomena [31]. Latent representations encoded by neural networks provide a new opportunity for measuring morphological similarity. In our similarity search evaluation, we measure the morphological similarity of galaxies by comparing feature embeddings through a similarity matrix. Specifically, we calculate pairwise similarities using dot products between feature vectors, creating a matrix where each entry indicates the similarity value between two galaxy images. For each image, we retrieve the most similar images (excluding the image itself) and use these to evaluate retrieval performance.

The comparison results of GalaxAlign and other methods evaluated in mAP@5 and mAP (mAP@all) are shown in Table 3. Our models demonstrate superior performance over baseline methods on both GalaxyMNIST and Galaxy10 datasets. While other fine-tuned general-purpose models show limited effectiveness, our approach, incorporating multi-modal alignment, outperforms traditional architectures, achieving better results in identifying galaxy morphological similarities. This result underscores our model’s capacity to adapt well to astronomical data.

The results in Figure 7 demonstrate that our model effectively retrieves galaxies with similar morphological characteristics to the query. Across various galaxy types, the top-ranked matches closely resemble the query galaxy’s shape and structure, indicating strong model performance in identifying morphological similarities.

4.5. Ablation Studies

We conduct an ablation study to evaluate the contribution of each alternative in our approach. First, we compare how our model works with ViT and ConvNeXT. Then we examine the effect of our tri-modality input in comparison with

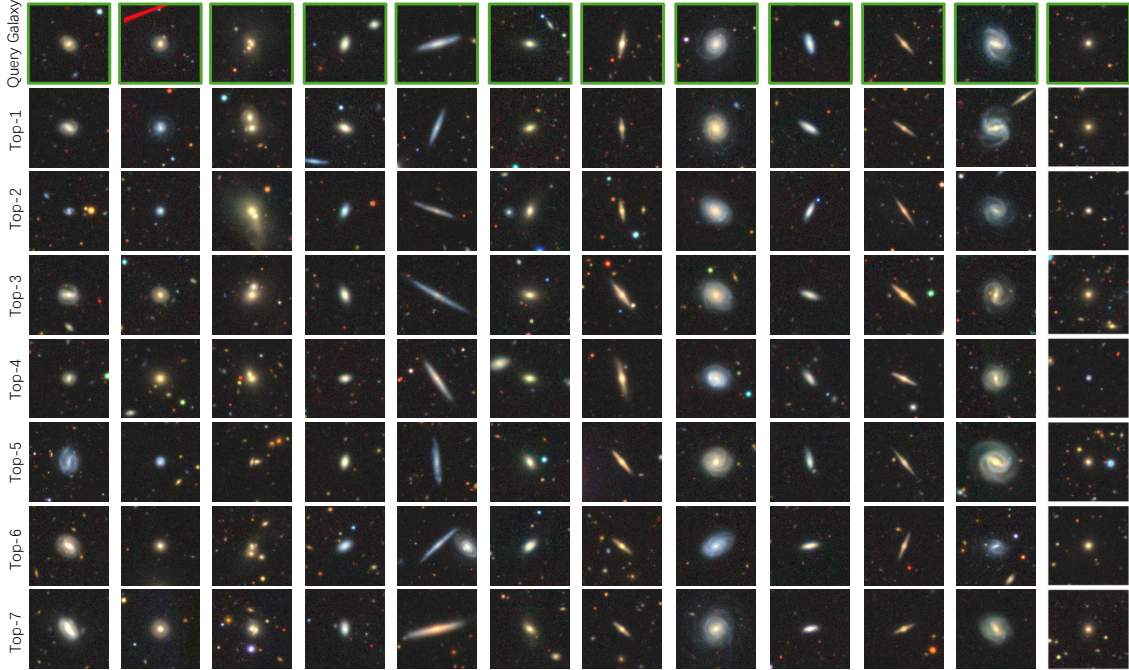


Figure 7. Examples of similarity search on the Galaxy10 dataset. The top row shows the query galaxy images (outlined in green) for each column, and the other rows display the seven most similar galaxies retrieved by the model.

the text-image bimodal CLIP model without the schematic symbol input. Finally, we compare our models across different stages of fine-tuning: Ours.v1 is the warm-up model trained through the first stage, omitting the second training stage; Ours.v2 skips the first stage and directly goes into the second stage of training until convergence; Ours.v3 omits the second stage, training through the first stage to convergence; Ours.Scratch goes through both stages, but is trained from scratch on the Galaxy10 and GalaxyMNIST datasets, without pre-training on large-scale natural datasets.

The results in Table 4 show the impact of each alternative in our approach. The full models, Ours(ViT-16) and Ours(ConvNeXT), achieve the highest accuracy and F1 scores on both datasets. Removing the symbol modality (CLIP models) or omitting training stages (e.g., Ours.v1, Ours.v2, and Ours.v3) reduces performance. The Ours.Scratch variant, trained without pretraining, shows notable drops, indicating the impact of pretraining with large-scale general datasets on astronomy tasks.

5. Conclusion and Future Work

In this paper, we introduced GalaxAlign, a tri-modal framework designed to finetune vision foundation models for galaxy morphology analysis, effectively utilizing schematic symbols, text descriptions, and galaxy images. By integrating domain-specific knowledge in a multi-modal approach, GalaxAlign effectively reuses the general foundation mod-

Table 4. Ablation Study Results on Classification Task

Model Variant	Galaxy10		GalaxyMNIST	
	Accuracy	F1	Accuracy	F1
CLIP(ViT-16)	0.9635	0.9549	0.9125	0.9129
Ours.v1 (ViT-16)	0.9457	0.9398	0.9125	0.9132
Ours.v2 (ViT-16)	0.9647	0.9607	0.8965	0.8967
Ours.v3 (ViT-16)	0.9678	0.9624	0.9245	0.9247
Ours.Scratch(ViT-16)	0.9585	0.9558	0.8620	0.8621
Ours(ViT-16)	0.9732	0.9702	0.9272	0.9276
CLIP(ConvNeXT)	0.9625	0.9537	0.9310	0.9316
Ours.v1 (ConvNeXT)	0.9428	0.9330	0.8600	0.8596
Ours.v2 (ConvNeXT)	0.9656	0.9593	0.9260	0.9266
Ours.v3 (ConvNeXT)	0.9651	0.9607	0.9360	0.9365
Ours.Scratch(ConvNeXT)	0.9599	0.9568	0.9301	0.9236
Ours(ConvNeXT)	0.9710	0.9664	0.9372	0.9377

els pre-trained on natural datasets and reduces the need for manually labeled data for training foundation models from scratch.

While GalaxAlign is designed for galaxy data, the multi-modal framework—integrating images, textual descriptions, and schematic symbols—is well-suited to other natural sciences such as biology for cellular and species classification, or geology for analyzing mineral structures, where both structure and descriptive information are essential and available.

References

- [1] Mahmoud Assran, Mathilde Caron, Ishan Misra, Piotr Bojanowski, Florian Bordes, Pascal Vincent, Armand Joulin, Mike Rabbat, and Nicolas Ballas. Masked siamese networks for label-efficient learning. In *European Conference on Computer Vision*, pages 456–473. Springer, 2022. 2, 4, 5, 6, 7
- [2] Robert D Blum, Kaylan Burleigh, Arjun Dey, David J Schlegel, Aaron M Meisner, Michael Levi, Adam D Myers, Dustin Lang, John Moustakas, Anna Patej, et al. The decam legacy survey. In *American Astronomical Society Meeting Abstracts# 228*, pages 317–01, 2016. 4
- [3] Micah Bowles, Hongming Tang, Eleni Vardoulaki, Emma L Alexander, Yan Luo, Lawrence Rudnick, Mike Walmsley, Fiona Porter, Anna MM Scaife, Inigo Val Slijepcevic, et al. A new task: Deriving semantic class targets for the physical sciences. In *NeurIPS 2022 Machine Learning and the Physical Sciences Workshop*, 2022. 1, 3
- [4] Micah Bowles, Hongming Tang, Eleni Vardoulaki, Emma L Alexander, Yan Luo, Lawrence Rudnick, Mike Walmsley, Fiona Porter, Anna MM Scaife, Inigo Val Slijepcevic, et al. Radio galaxy zoo emu: towards a semantic radio galaxy morphology taxonomy. *Monthly Notices of the Royal Astronomical Society*, 522(2):2584–2600, 2023. 1, 3
- [5] Jia Deng, Wei Dong, Richard Socher, Li-Jia Li, Kai Li, and Li Fei-Fei. Imagenet: A large-scale hierarchical image database. In *2009 IEEE conference on computer vision and pattern recognition*, pages 248–255. Ieee, 2009. 5
- [6] Arjun Dey, David J Schlegel, Dustin Lang, Robert Blum, Kaylan Burleigh, Xiaohui Fan, Joseph R Findlay, Doug Finkbeiner, David Herrera, Stéphanie Juneau, et al. Overview of the desi legacy imaging surveys. *The Astronomical Journal*, 157(5):168, 2019. 4
- [7] Sander Dieleman, Kyle W Willett, and Joni Dambre. Rotation-invariant convolutional neural networks for galaxy morphology prediction. *Monthly notices of the royal astronomical society*, 450(2):1441–1459, 2015. 1
- [8] Alexey Dosovitskiy. An image is worth 16x16 words: Transformers for image recognition at scale. *arXiv preprint arXiv:2010.11929*, 2020. 2, 5, 6, 7
- [9] Kaiming He, Xiangyu Zhang, Shaoqing Ren, and Jian Sun. Deep residual learning for image recognition. In *Proceedings of the IEEE conference on computer vision and pattern recognition*, pages 770–778, 2016. 2, 5, 6, 7
- [10] Kaiming He, Xinlei Chen, Saining Xie, Yanghao Li, Piotr Dollár, and Ross Girshick. Masked autoencoders are scalable vision learners. In *Proceedings of the IEEE/CVF conference on computer vision and pattern recognition*, pages 16000–16009, 2022. 2, 4, 5, 6, 7
- [11] Leung Henry. Galaxy10 decals dataset. <https://github.com/henrysky/Galaxy10>, 2021. 1, 4
- [12] Gabriel Ilharco, Mitchell Wortsman, Ross Wightman, Cade Gordon, Nicholas Carlini, Rohan Taori, Achal Dave, Vaishaal Shankar, Hongseok Namkoong, John Miller, Hananeh Hajishirzi, Ali Farhadi, and Ludwig Schmidt. Openclip, 2021. If you use this software, please cite it as below. 4
- [13] Raza Imam, Mohammed Talha Alam, Umaima Rahman, Mohsen Guizani, and Fakhri Karray. Cosmoclip: Generalizing large vision-language models for astronomical imaging. *arXiv preprint arXiv:2407.07315*, 2024. 3
- [14] Manuel Jiménez, Emilio J Alfaro, Mercedes Torres Torres, and Isaac Triguero. Czsl: Learning from citizen science, experts, and unlabelled data in astronomical image classification. *Monthly Notices of the Royal Astronomical Society*, 526(2):1742–1756, 2023. 2
- [15] Francois Lanusse, Liam Holden Parker, Siavash Golkar, Alberto Bietti, Miles Cranmer, Michael Eickenberg, Geraud Krawezik, Michael McCabe, Ruben Ohana, Mariel Pettee, et al. Astroclip: cross-modal pre-training for astronomical foundation models. In *NeurIPS 2023 AI for Science Workshop*, 2023. 1, 2, 3
- [16] Chris Lintott, Kevin Schawinski, Steven Bamford, Anže Slosar, Kate Land, Daniel Thomas, Edd Edmondson, Karen Masters, Robert C Nichol, M Jordan Raddick, et al. Galaxy zoo 1: data release of morphological classifications for nearly 900 000 galaxies. *Monthly Notices of the Royal Astronomical Society*, 410(1):166–178, 2011. 1, 3
- [17] Shengchao Liu, Yanjing Li, Zhuoxinran Li, Anthony Gitter, Yutao Zhu, Jiarui Lu, Zhao Xu, Weili Nie, Arvind Ramanathan, Chaowei Xiao, et al. A text-guided protein design framework. *arXiv preprint arXiv:2302.04611*, 2023. 3
- [18] Siddharth Mishra-Sharma, Yiding Song, and Jesse Thaler. Paperclip: Associating astronomical observations and natural language with multi-modal models. *arXiv preprint arXiv:2403.08851*, 2024. 3
- [19] Maxime Oquab, Timothée Darcet, Théo Moutakanni, Huy Vo, Marc Szafraniec, Vasil Khalidov, Pierre Fernandez, Daniel Haziza, Francisco Massa, Alaaeldin El-Nouby, et al. Dinov2: Learning robust visual features without supervision. *arXiv preprint arXiv:2304.07193*, 2023. 2, 4, 5, 6, 7
- [20] Alec Radford, Jong Wook Kim, Chris Hallacy, Aditya Ramesh, Gabriel Goh, Sandhini Agarwal, Girish Sastry, Amanda Askell, Pamela Mishkin, Jack Clark, et al. Learning transferable visual models from natural language supervision. In *International conference on machine learning*, pages 8748–8763. PMLR, 2021. 2, 3
- [21] Olga Russakovsky, Jia Deng, Hao Su, Jonathan Krause, Sanjeev Satheesh, Sean Ma, Zhiheng Huang, Andrej Karpathy, Aditya Khosla, Michael Bernstein, et al. Imagenet large scale visual recognition challenge. *International journal of computer vision*, 115:211–252, 2015. 1
- [22] Ana Sanchez-Fernandez, Elisabeth Rumetshofer, Sepp Hochreiter, and Günter Klambauer. Cloome: contrastive learning unlocks bioimaging databases for queries with chemical structures. *Nature Communications*, 14(1):7339, 2023. 3
- [23] David R Silva, Robert D Blum, Lori Allen, Arjun Dey, David J Schlegel, Dustin Lang, John Moustakas, Aaron M Meisner, Francisco Valdes, Anna Patej, et al. The mayall z-band legacy survey. In *American Astronomical Society Meeting Abstracts# 228*, pages 317–02, 2016. 4
- [24] Inigo V Slijepcevic, Anna MM Scaife, Mike Walmsley, Micah Bowles, O Ivy Wong, Stanislav S Shabala, and

- Sarah V White. Radio galaxy zoo: towards building the first multipurpose foundation model for radio astronomy with self-supervised learning. *RAS Techniques and Instruments*, 3(1):19–32, 2024. 1
- [25] Laurens Van der Maaten and Geoffrey Hinton. Visualizing data using t-sne. *Journal of machine learning research*, 9 (11), 2008. 5
- [26] Vicente Vivanco Cepeda, Gaurav Kumar Nayak, and Mubarak Shah. Geoclip: Clip-inspired alignment between locations and images for effective worldwide geolocalization. *Advances in Neural Information Processing Systems*, 36, 2024. 3
- [27] S Voloshynovskyy. Vision foundation models: can they be applied to astrophysics data? *arXiv preprint arXiv:2409.11175*, 2024. 1, 2, 4, 6
- [28] Mike Walmsley. Galaxy mnist dataset. https://github.com/mwalmsley/galaxy_mnist, 2022. 4
- [29] Mike Walmsley, Lewis Smith, Chris Lintott, Yarin Gal, Steven Bamford, Hugh Dickinson, Lucy Fortson, Sandor Kruk, Karen Masters, Claudia Scarlata, et al. Galaxy zoo: probabilistic morphology through bayesian cnns and active learning. *Monthly Notices of the Royal Astronomical Society*, 491(2):1554–1574, 2020. 1, 2
- [30] Mike Walmsley, Chris Lintott, Tobias Géron, Sandor Kruk, Coleman Krawczyk, Kyle W Willett, Steven Bamford, Lee S Kelvin, Lucy Fortson, Yarin Gal, et al. Galaxy zoo decals: Detailed visual morphology measurements from volunteers and deep learning for 314 000 galaxies. *Monthly Notices of the Royal Astronomical Society*, 509(3):3966–3988, 2022. 2, 3, 4, 5
- [31] Mike Walmsley, Anna MM Scaife, Chris Lintott, Michelle Lochner, Verlon Etsebeth, Tobias Géron, Hugh Dickinson, Lucy Fortson, Sandor Kruk, Karen L Masters, et al. Practical galaxy morphology tools from deep supervised representation learning. *Monthly Notices of the Royal Astronomical Society*, 513(2):1581–1599, 2022. 1, 2, 7
- [32] Mike Walmsley, Campbell Allen, Ben Aussel, Micah Bowles, Kasia Gregorowicz, Inigo Val Slijepcevic, Chris J Lintott, Anna M Scaife, Maja Jabłońska, Kosio Karchev, et al. Zoobot: Adaptable deep learning models for galaxy-morphology. *Journal of Open Source Software*, 8(85), 2023. 5, 7
- [33] Mike Walmsley, Tobias Géron, Sandor Kruk, Anna MM Scaife, Chris Lintott, Karen L Masters, James M Dawson, Hugh Dickinson, Lucy Fortson, Izzy L Garland, et al. Galaxy zoo desi: Detailed morphology measurements for 8.7 m galaxies in the desi legacy imaging surveys. *Monthly Notices of the Royal Astronomical Society*, 526(3):4768–4786, 2023. 2
- [34] Kyle W Willett, Chris J Lintott, Steven P Bamford, Karen L Masters, Brooke D Simmons, Kevin RV Casteels, Edward M Edmondson, Lucy F Fortson, Sugata Kaviraj, William C Keel, et al. Galaxy zoo 2: detailed morphological classifications for 304 122 galaxies from the sloan digital sky survey. *Monthly Notices of the Royal Astronomical Society*, 435(4): 2835–2860, 2013. 1, 3
- [35] The Galaxy Zoo. Galaxy zoo classification. <https://www.zooniverse.org/projects/zookeeper/galaxy-zoo/classify>, 2024. Nov. 2024. 2, 3
- [36] Hu Zou, Xu Zhou, Xiaohui Fan, Tianmeng Zhang, Zhimin Zhou, Jundan Nie, Xiyan Peng, Ian McGreer, Linhua Jiang, Arjun Dey, et al. Project overview of the beijing–arizona sky survey. *Publications of the Astronomical Society of the Pacific*, 129(976):064101, 2017. 4